Kinetic simulation of vapor deposition and growth

P. W. Rooney and F. Hellman
Department of Physics, University of California at San Diego, La Jolla, California 92093
(Received 11 January 1993)

We present a stochastic Monte Carlo model of vapor deposition and growth of a crystalline, binary, A_3B metallic alloy with a negative energy of mixing. Our model incorporates deposition and surface diffusion in a physically correct manner and allows us to simulate deposition rates that are experimentally realizable. We examine the effects of deposition rate and temperature on the development of short-range order (SRO) in the as-deposited film. We see SRO increase with temperature, but we see no corresponding development of anisotropic SRO (preferential ordering of A-B pairs along the growth direction).

It is well known that surface diffusion rates are many orders of magnitude higher than bulk diffusion rates[1] at the same temperature. Thus, a growing surface during thin-film deposition is inherently anisotropic as diffusion is effectively limited to the surface of the film. We are interested in investigating whether the presence of this anisotropy during growth could manifest itself in a pair ordering anisotropy (e.g., preferred orientation of A-B pairs out of the film plane) in the resulting film of a vapor-deposited A-B alloy.

This investigation is motivated in part by the observed growth-induced magnetic anisotropy in amorphous rare-earth–transition-metal (R-M) alloys, the magnitude of which increases with increasing deposition temperature, unlike what would be expected of nonequilibrium effects such as shadowing or columnar microstructure.[2,3] This anisotropy is frequently attributed to a so-called pair ordering of R-M pairs along the growth direction.

A pair ordering anisotropy might be induced in a binary alloy with a negative energy of mixing in the following manner: an atom of type B is deposited and diffuses along the surface. This mobile adatom will spend more time at sites that have a higher fraction of neighbors of the opposite type (in this case, A). This preferred local configuration would get frozen into the bulk by the deposition of further adatoms from the vapor. For a lattice such as (100) oriented fcc, where a surface atom adding to an incomplete layer would have more neighbors in the layer below than in its own layer, the freezing in of the A atom in a B-rich pocket would lead to a greater number of A-B pairs oriented out of the film plane.

The pair ordering mechanism described above involves competition between surface diffusion rates and the deposition rate. The adatoms must have time to sample their local environment before they are buried by additional adlayers. At the same time, deposition rates in the laboratory are not infinitesimally low and the growing surface does not have time to fully equilibrate before another adlayer is deposited. We would expect the microstructure of the resulting film to reflect the kinetic evolution of the system during growth and it is important to develop a simulation scheme that follows this kinetic pathway. Unfortunately, molecular-dynamics simulations are constrained by computing speed to minimum deposition rates of about a monolayer (ML)/ns whereas physically realistic rates are on the order of one ML/s. We have developed a stochastic Monte Carlo[4–7] simulation model that mimics the dynamics of film growth but does not follow it explicitly. In our model, an atom is deposited on the surface and then all surface atoms attempt to move sequentially into neighboring vacancies before another atom is deposited. Bulk vacancies, overhangs, and reevaporation during the diffusion step are all allowed. The probability that any attempted move is successful is proportional to $\exp(-E/k_BT)$, where E is the height of the kinetic barrier separating an atom from its nearest-neighbor vacancy. The procedure is Monte Carlo-like in that atoms are moved "by hand" among sites on a predetermined lattice, but use of the transition state energy to determine the success rate of a given hop ensures that the kinetic evolution of the growing film is reproduced.

The difference between our model and previous stochastic Monte Carlo models lies in the manner in which the magnitude of the kinetic barrier E, separating initial and final sites of a mobile atom, is determined. Previous models have relied primarily on the coordination of the initial site to determine E. However, the true transition state energy depends on the coordination of both the initial site and the final site. In our model, empirical interatomic potentials are used to calculate the binding energy of the mobile atom when it is in the saddle position between the initial and final site. The barrier E is taken to be the difference in binding energy between the initial site and the saddle position and thus depends in part on the coordination of the final site. Our model is an extension of the stochastic kinetic simulation (SKS) developed by Lu and Metiu.[8–10]

We chose to model growth on a fcc lattice as attempting to simulate the growth of an amorphous material would have been computationally intractable and the fcc lattice, being a close-packed structure, is a better representation of a dense-packed amorphous film than other crystal systems. This model is closely related to growth of an Ising antiferromagnet except that vacancies are allowed. Vacancies necessarily have a strong influence in

0163-1829/93/48(5)/3079(6)/$06.00 ©1993 The American Physical Society

this kinetic model even though the completed film possesses, on average, zero vacancies in the bulk. It is well known that an Ising antiferromagnet on a fcc lattice is frustrated and that its ground state is highly degenerate although considerably less so than an Ising antiferromagnet on a two-dimensional (2D) triangular lattice.[11] The fcc Ising antiferromagnet orders at low temperatures[12–14] despite the ground-state degeneracy. The ordering is deemed to be weak in the sense that the free-energy difference that drives the transition is small and the ordered phase is not unique; there are six energetically equivalent periodic structures to which the system can order.

The A_3B stoichiometry which we have chosen for our model is known, in real materials such as Cu_3Au, to lift the degeneracy of the ground state and to allow the system to exhibit long-range order with B atoms at the corner sites and A atoms at the faces,[15] but this ordering cannot occur through nearest-neighbor interactions exclusively[16] (this conclusion is easiest to understand by considering the fact that in the ordered phase, the {200} planes are populated exclusively by atoms of type A). The pure Ising model, with nearest-neighbor interactions only, similar to what we have chosen for our simulation, does not exhibit perfect long-range order even with three to one stoichiometry. In our growth model, the free energy is minimized by adatoms incorporating at sites that maximize the number of antiferromagnetic bonds; the global (bulk) free energy of the completed film would be reached only by extensive annealing and would presumably show the weak ordering discussed above. The frustration inherent in the fcc lattice means that other configurations, including an anisotropic arrangement of A-B pairs, cost less free energy than they would in an unfrustrated system such as simple cubic or body-centered cubic. It is worth pointing out that perfect long-range order is incompatible with anisotropic short-range order (anisotropic pair ordering) as anisotropy in the short-range order breaks the symmetry required for the long-range ordered phase.

In our simulation, atoms are deposited at normal incidence with a sticking coefficient of 1 on to a (100) oriented fcc lattice. The lattice positions are rigidly fixed and there is no allowance for size differences between A and B atoms. We have chosen the (100) orientation because, of the low-index planes, (100) has the maximum number of interplane bonds and, therefore, we might expect an enhanced out-of-plane pair ordering anisotropy.

The deposition step is followed by a relaxation step in which the last adatom gives up its condensate energy. Relaxation is then followed by a diffusion step in which some fraction (possibly greater than 1) of surface atoms attempt to move into neighboring vacancies. In this model, an atom is defined to be in the surface if it has at least one nearest-neighbor vacancy. Thus, atoms that are far below the solid-vapor interface may still have some mobility. The diffusion step is followed by the deposition of another adatom and the cycle is repeated. The simulated deposition rate is determined by the number of attempts that are made during the diffusion step before another adatom is deposited. The normalization factor used to convert the simulated attempt frequency into time is chosen to match the simulated surface diffusion rate to the experimentally observed value for surface self-diffusion on (100) Cu at 500 K.[17,18]

We assume that diffusion takes place via a series of uncorrelated jumps to nearest-neighbor vacancies. Multiple jumps or long jumps to distant sites are not allowed. The assumption is reasonable as long as the temperature is less than 0.5 T_m, where T_m is the melting temperature.[19,20] We assume further that only nearest-neighbor interactions are significant when calculating the height of the barrier separating an atom from its neighboring vacancy and that pairwise spherical potentials are adequate for describing metallic bonding. Each interatomic bond (A-A, B-B, or A-B) is represented by a Morse potential

$$V(r)=D(e^{-2a|r-r_0|}-2e^{-a|r-r_0|}) , \quad (1)$$

using values of the Morse parameters fit to Cu by Ayrault:[21] $a=1.392$ Å, $r_0=2.838$ Å; $D=D_0=0.3446$ eV for A-A and B-B bonds. These values result in a lattice spacing of 3.597 Å (fcc lattice) and a cohesive energy of 3.478 eV /atom.

For A-B bonds, $D=D_0+\varepsilon$, where ε is the energy of mixing. In general, the energy of mixing is defined as follows:

$$\varepsilon=\varepsilon_{AB}-(\varepsilon_{AA}+\varepsilon_{BB})/2 \quad (2)$$

In this simulation, $\varepsilon_{AA}=\varepsilon_{BB}=D_0$ and ε is an adjustable parameter. Typically, for binary metals alloys ε will be on the order of a few hundredths of an eV.

Each atom in the surface is surrounded by 12 nearest-neighbor (NN) sites, each having three possible occupation states: A, B, or unoccupied. Similarly, a vacant site is surrounded by 12 NN sites. A surface atom and its NN vacancy share four NN sites and, thus, there are a total of 18 sites neighboring a surface atom and one of its NN vacancies (the surface atom and its NN vacancy are neighbors to each other and are excluded from this count). The occupation states of these 18 neighboring sites define an energy surface that links the initial and final site of the mobile atom. The energy surface will contain one or more saddle points through which the mobile atom must pass during the course of its jump. The barrier crossing rate will be a weighted sum of the crossing rates associated with each individual saddle point. In practice, the lowest (energy) saddle will determine the crossing rate and the other paths available to the mobile atom may be safely ignored. The height of the kinetic barrier separating the surface atom and its neighboring vacancy is given by

$$E=\sum_j [V(r_j^{\text{saddle}})-V(r_j^{\text{initial}})] , \quad (3)$$

where j runs over the lattice positions neighboring the initial and final sites. r_j^{saddle} is the separation between the mobile atom when it is at the saddle point and the atom, if any, at the jth neighboring site.

When calculating the energy of the transition state, the neighboring atoms are taken to be fixed at their equilibrium positions. In a real system these atoms would be per-

turbed by the movement of the mobile atom into the saddle point. The perturbation of the surrounding lattice would, in turn, affect the energy of the transition state. However, the energy associated with the dynamical correction is small[22,23] relative to the other energies in the problem (energy of mixing, etc.) and we ignore it.

In the absence of dynamical corrections, the determination of the barrier height is relatively straightforward. The potential final site (NN vacancy) has already been selected stochastically and the path to that site is determined by the occupation states of the surrounding sites. In the case of bulk diffusion, the diffusion path is simply a straight-line path to the vacancy and the barrier height is the maximum value of E in Eq. (3) along that path.[24] In the case of surface diffusion, the path is not a straight line, but rather an arc, as the mobile atom moves up out of one pocket of neighboring atoms and down into another. Each unique configuration of surface atom, NN vacancy, and their neighbors will have a unique path associated with it. For each configuration, our program makes an educated guess and selects a tube within which the true path should lie. Many possible paths within this tube are traversed and in each case a maximum value of E is calculated. The *lowest* of these values is taken to be the height of the kinetic barrier separating the initial and final sites. The Morse potential has no repulsive core; instead, atoms are allowed to come no closer than λ, the nearest-neighbor distance, at any time during the jump. The values of E are calculated *a priori* and stored in a lookup table (this table has on the order of 10^7 entries due to the large number of possible configurations). The table entries are accessed during the simulation.

In a typical simulation run, 20 layers with 50 sites per layer are deposited. Periodic boundary conditions are imposed in x and y where the x-y plane is the film plane and z is the growth direction. We check for finite-size effects by occasionally simulating the growth of ten layers with 882 sites per layer and see no change in our results.

Once a film is grown, the short-range order is characterized by stepping through the lattice and counting the number and type of neighbors for each atom. From this count, the normalized Cowley short-range order parameter[25] α is calculated. α is defined as follows: $\alpha=[(P_{AA}-n_A)/(1-n_A)]/\alpha_0$ where P_{AA} is the (average) fraction of nearest-neighbor sites about an A atom occupied by A atoms and n_A is the atomic fraction of A atoms in the film. α_0 is the Cowley parameter for perfect short-range order ($\alpha_0=-1/3$ for an ordered A_3B alloy). Thus, $\alpha=0$ indicates a statistical distribution of A-B pairs, $\alpha=1$ indicates perfect short-range order, and $\alpha<0$ indicates clustering of like atoms. The anisotropic short-range order is characterized in the following manner: A = (the number of out-of-plane A-B pairs)/(the number of in-plane A-B pairs) -2. This definition yields $A=0$ for no directional order, $A>0$ if there is net out-of-plane pair ordering, and $A<0$ if there is net in-plane pair ordering. The subtraction of 2 is required in order to make the anisotropic short-range order parameter zero when there is no preferred orientation of A-B pairs [a fully coordinated (bulk) atom in a fcc (100) plane has eight bonds to neighbors out of the plane and four bonds to neighbors in the plane].

Figure 1 shows a plot of the short-range order in the simulated films as a function of deposition temperature for two different values of the energy of mixing: $\varepsilon=0.044$ eV (corresponding to a temperature of 511 K) and $\varepsilon=0.034$ eV (corresponding to a temperature of 395 K). The deposition rate is fixed at $R=1$ ML/s. In both cases, the short-range order *increases* with deposition temperature until the point at which the deposition temperature is comparable to the energy of mixing. Raising the deposition temperature facilitates diffusion and allows mobile atoms to find favorable sites. When the temperature becomes comparable to the energy of mixing, mobile atoms lose the ability to distinguish between sites that maximize A-B pairing and those that do not (but have the same coordination). As the deposition temperature is raised further, the resulting film becomes increasingly (chemically) disordered. In Fig. 1 and all subsequent plots, each point represents an average value of data from three or more simulation runs. The error bars reflect the spread in the data.

Figure 2 shows a plot of the *anisotropic* short-range order (SRO) parameter A as a function of deposition temperature. The deposition rate and the values of ε are the same as those used to generate the plot in Fig. 1. There is *no tendency* for A-B pairs to orient themselves either in or out of the film plane at any temperature, despite formation of A-B pairs. Varying the deposition rate and the energy of mixing affected the degree of grown-in short-range order in the films but had no affect on the anisotropic short-range order parameter.

Figure 3 shows a plot of short-range order as a function of deposition rate at two different temperatures, but the same value of ε ($\varepsilon=0.044$ eV). At 500 K, the temperature at which SRO reaches its maximum, there is a rather abrupt crossover to disordered growth as the deposition rate is raised above $R=10$ ML/s. In our model, the deposition rate sets an upper limit on the number of attempts a given surface atom will make at jumping to neighboring sites, whereas the temperature determines the success rate of those attempts. At 300 K, the cross-

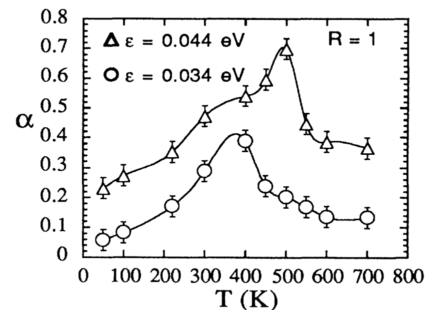

FIG. 1. Normalized short-range order α as a function of deposition temperature for two different values of the energy of mixing ε. SRO increases with T up to the point at which $k_BT\cong\varepsilon$. $\alpha=1$ indicates perfect short-range order (maximum A-B pairing) and $a=0$ indicates a statistical distribution of A-B pairs. The error bars reflect the spread in the data over three or more simulation runs.

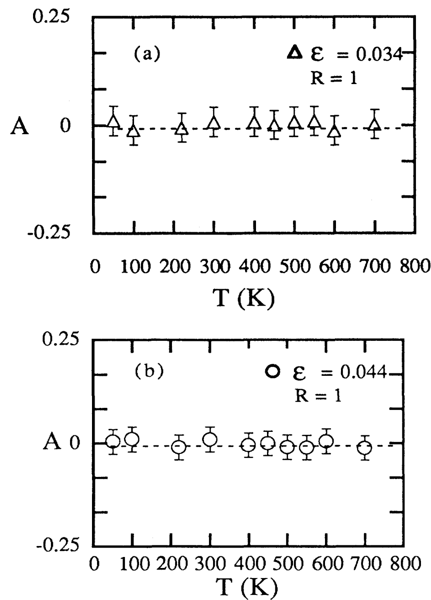

FIG. 2. Anisotropic short-range order as a function of temperature for two different values of the energy of mixing: (a) $\varepsilon=0.034$ eV, (b) $\varepsilon=0.044$ eV. Although in both cases SRO increased with T up to $T\cong\varepsilon/k_B$ (Fig. 1), there is no corresponding development of anisotropic short-range order.

over to disordered growth is more gradual.

The effect of deposition rate and temperature on surface-atom mobility is further illustrated in Fig. 4. Here we show a plot of diffusion length, in units of the nearest-neighbor distance λ as a function of temperature for two different deposition rates. The diffusion length is the average distance (in the x-y plane) an adatom migrates from the site at which it was deposited until it is buried by the next adlayer. The diffusion exhibits Arrhenius-like behavior with an activation energy of 0.96 eV. Here, the activation energy is a measure of the average kinetic barrier height; this value closely matches the expected value of the activation energy for surface self-diffusion on (100) Cu of 1 eV.[26]

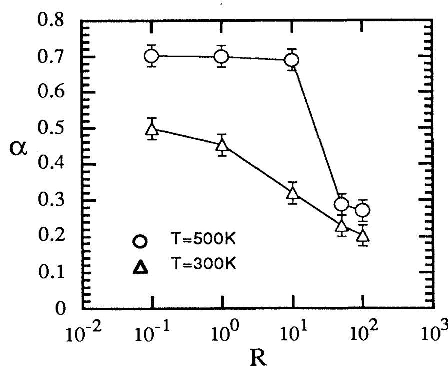

FIG. 3. Short-range order as a function of deposition rate R at two different deposition temperatures. In both cases $\varepsilon=0.044$ eV. SRO decreases as R increases. The transition to the disordered state is more pronounced at $T=500$ K. This is also the temperature at which α reaches a maximum (for the given value of ε).

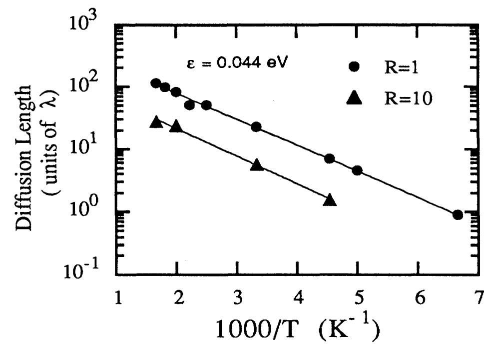

FIG. 4. Diffusion length (average distance an adatom migrates over the surface before it is buried by the next adlayer) in units of λ, the nearest-neighbor distance, as a function of deposition temperature. Data are shown for two different values of the deposition rate R.

Figure 5 shows a plot of surface roughness of the resulting film (at the end of the deposition) as a function of deposition temperature for two different values of the deposition rate (film thickness is fixed). The roughness σ is characterized by the rms variance in the height and is defined by

$$\sigma^2=\frac{1}{n}\sum_{j=1}^{n}(h_j-\bar{h})^2 , \tag{4}$$

where n is the number of lattice sites in one layer. As expected, roughness decreases with increasing deposition temperature (the system is well below the equilibrium roughening temperature) and decreasing deposition rate.

For most of the simulation runs, the diffusion length exceeds the width of the surface. The surface is $\sqrt{2n}\,\lambda$ on a side, where n is the number of sites in a layer and λ is the nearest-neighbor distance; thus, for $n=50$, the width is 10λ, and for $n=882$, the width is 42λ. We have, however, repeated these simulations on a larger lattice ($n=10\,082$; each layer is 142λ on a side) and have seen no change in any of the properties of the resulting films, i.e.,

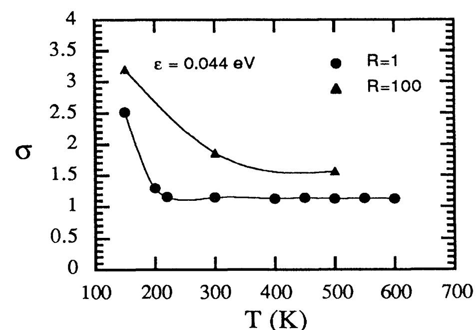

FIG. 5. Rms roughness of the surface of the resulting film (after deposition has stopped) as a function of deposition temperature for two different values of the deposition rate R.

short-range order, anisotropic short-range order, and roughness.

At deposition temperatures below 200 K, adatom mobility is dependent on the details of the relaxation step (in the context of our model, they are unimportant above 200 K as thermally activated surface diffusion overwhelms any effect due to the condensate energy). Even at low temperatures, the last adatom retains some mobility after deposition until it gives up its condensate energy to the lattice. Our relaxation algorithm is as follows: we assume a condensate energy of 3.4 eV (energy of sublimation for Cu)[27] and allow the adatom to thermally equilibrate with the lattice according to Newton's law of cooling,

$$T=\Delta T \exp(-t/t_c)+T_L \ , \tag{5}$$

where $\Delta T=T_0-T_L$, $T_0=E_{\text{condensate}}/k_B=2.6\times10^4$ K, and T_L is the lattice temperature. t_c is a parameter which characterizes how quickly the adatom equilibrates to the lattice temperature. In this case, $t_c=5\times10^{-14}$ s.[21] The attempt frequency for hopping to neighboring sites is chosen to be $\nu=k_BT/\hbar$, the average vibrational frequency of a surface atom. e.g., $\nu\cong5\times10^{15}$ Hz at $k_BT=3.4$ eV so that, at this temperature, the adatom can make several hops before its temperature drops by a factor of $1/e$. The probability that a given attempt will be successful is proportional to $\exp(-E/k_BT)$, as before.

We found that films grown at low temperature exhibited a small degree of short-range order due to the adatom mobility imparted by the condensate energy, but once again there was *no* preference for *A*-*B* pairs to form preferentially either in or out of the film plane. The precise degree of short-range order formed in these simulated films grown below 200 K depends sensitively on parameters such as t_c and ν, but in all cases the anisotropic short-range order was zero.

In conclusion, we have developed a stochastic Monte Carlo simulation of thin-film growth in order to explore the possibility of a surface mediated grown-in pair ordering anisotropy. We saw an increase in short-range order up to the point at which the deposition temperature was comparable to the energy of mixing, but we saw no evidence of anisotropic short-range order. It seems likely, therefore, that the growth-induced magnetic anisotropy in the amorphous rare-earth–transition-metal films is fundamentally linked to their noncrystalline structure.

We would like to thank George Gilmer, Herbert Levine, Ivan Schuller, and Tim Moran for useful discussions. This work has been supported by the AFOSR (Grant No. 89-0432) and the National Science Foundation through the San Diego Supercomputer Center.

---

[1] C. P. Flynn, J. Phys. F. **18**, L195 (1988).

[2] N. Heiman, A. Onton, D. F. Kyser, K. Lee, and C. R. Guarnieri, in *Magnetism and Magnetic Materials,* AIP Conf. Proc. No. XXIV, edited by C. D. Graham Jr., G. H. Lander, and J. J. Rhyne (AIP, New York, 1975), p. 573.

[3] F. Hellman and E. M. Gyorgy, Phys. Rev. Lett. **68**, 1391 (1992), and references therein.

[4] I. K. Marmorkos and S. Das Sarma, Surf. Sci. **237**, L411 (1990).

[5] R. Kariotis and M. G. Lagally, Surf. Sci. **216**, 557 (1989).

[6] S. Clarke and D. Vvedensky, Phys. Rev. Lett. **58**, 2235 (1987).

[7] S. Clarke and D. Vvedensky, Surf. Sci. **189-190**, 1033 (1987).

[8] Yan-Ten Lu and Horia Metiu, Surf. Sci. **245**, 150 (1991).

[9] Yan-Ten Lu and Horia Metiu, Surf. Sci. **254**, 209 (1991).

[10] Yan-Ten Lu, Pierre Petroff, and Horia Metiu, Appl. Phys. Lett. **57**, 2683 (1990).

[11] A. Danielian, Phys. Rev. **133** (1964).

[12] R. Bidaux, J. P. Carton, R. Conte, and J. Villain, in *Disordered Systems and Localization,* edited by C. Castellani *et al.*, Lecture Notes in Physics Vol. 149 (Springer-Verlag, New York, 1981), p. 161.

[13] J. Slawny, J. Stat. Phys. **20**, 711 (1979).

[14] Danielian (see Ref. 11) and Slawney (see Ref. 13) have shown that a fcc Ising antiferromagnet orders at low temperature even though there is no long-range order at $T=0$. Although it seems paradoxical that at exactly $T=0$ there is no long-range order while at finite temperature there is a transition to an ordered phase, this is indeed the case for the equilibrium model. Of the many degenerate ground-state configurations possible at $T=0$, some are ordered and the excited states associated with these ordered configurations have higher entropy than the excited states associated with the disordered ground-state configurations. At finite but low temperature, the ordered configurations are selected out by the entropy term in the free energy. Danielian has also pointed out that even at $T=0$ the system exhibits partial long-range order in the sense that the ground-state configuration of any one of the triangular $\{111\}$ planes in the fcc structure is much less degenerate than a 2D triangular Ising antiferromagnet and the configuration of any one of these planes uniquely determines the configuration of the whole lattice.

[15] C. S. Barrett and T. B. Massalski, *Structure of Metals,* 3rd ed. (McGraw-Hill, New York, 1966), p. 272.

[16] M. K. Phani, Joel L. Lebowitz, and M. H. Kalos, Phys. Rev. B **21**, 4027 (1980).

[17] The clock in the simulation is the average number of attempted moves a typical surface atom makes between the deposition of subsequent monolayers. Let $R\equiv$ the deposition rate, $\eta\equiv$ the total number of attempted moves made between the deposition of subsequent adatoms, and $n\equiv$ the average number of atoms in the surface. Then the average number of attempted moves made by a typical surface atom between the deposition of subsequent adatoms is given by η/n. Since n atoms are deposited per monolayer, the number of attempted moves made by a typical surface atom between the deposition of subsequent monolayers is given by $(\eta/n)n$ which is simply equal to η. The deposition rate, then, can be expressed as $R=\chi/\eta$, where χ is a temperature-dependent normalization factor chosen in such a way as to match the simulated surface diffusion rate at $T=500$ K to that observed for (100) Cu at the same temperature.

The value of χ was chosen in the following manner: a single Cu atom diffusing on a smooth (100) Cu surface at $T=500$ K migrates approximately 330 Å/s (see Ref. 18). The diffusion of a single Cu adatom on a smooth (100) surface at $T=500$ K was simulated and the average number of attempts required

for the adatom to diffuse 330 Å (133λ where $\lambda=2.5$ Å, the nearest-neighbor spacing) was found to be 6×10^5. Therefore, at 500 K, 6×10^5 attempts corresponds to 1 s. At other temperatures, it is necessary to account for the fact that the actual attempt frequency for surface diffusion is proportional to $k_B T/\hbar$, the average vibrational frequency of a surface atom (see Refs. 6 and 7). Therefore, for a given deposition rate, the number of moves attempted by a real surface adatom scales with T [a factor independent of the success of the attempt, which scales with $\exp(-E/k_B T)$]. For a given deposition rate in ML/s, the number of simulated attempts during the diffusion step before another adatom is deposited, must also be scaled with T. The normalization factor χ, which converts the number of simulated attempts into 1/s, is thus equal to $6\times10^5 T/500$ K.

[18] F. Delamare and G. E. Rhead, Surf. Sci. **28**, 267 (1971).

[19] P. Shewmon, *Diffusion in Solids* (Minerals, Metals, & Materials Society, Warrendale, PA, 1989), p. 218.

[20] Gert Ehrlich and Kaj Stolt, Ann. Rev. Phys. Chem. **31**, 603 (1980).

[21] Guy Ayrault, Ph.D. thesis, University of Illinois, 1974.

[22] M. Marchese, G. Jacucci, and C. P. Flynn, Phys. Rev. B **36**, 9461 (1987).

[23] G. DeLorenzi, C. P. Flynn, and G. Jacucci, Phys. Rev. B **30**, 5430 (1984).

[24] In order for bulk diffusion to occur, the four shared neighbors between the initial site and the neighboring vacancy must move out of the way. These neighbors have no effect on the transition state energy as their separation from the mobile atom does not increase during the jump. However, the correlated motion necessary for bulk diffusion is unlikely and the attempt frequency is reduced by a factor of 10^4 in our simulation in order to match the rate of bulk self-diffusion in copper.

[25] J. M. Cowley, J. Appl. Phys. **21**, 24 (1950).

[26] P. Wynblatt and N. A. Gjostein, Surf. Sci. **12**, 109 (1968).

[27] Charles A. Wert, in *The Encyclopedia of Physics,* 3rd ed., edited by Robert M. Besancon (Van Nostrand, Reinhold, NY, 1985), p. 1144.